Supporting Information

Deep eutectic solvothermal synthesis NiS_2/CdS for visible light driven valorization of biomass intermediate 5-hydroxymethylfurfural (HMF) integrated with H_2 Production

Shuzi Liu,[a] Baolong Zhang,[a] Zhaohui Yang,[a] Zhimin Xue[*b], Tiancheng Mu[*a]

1. Experimental Section

1.1. Synthesis of sulfides nanostructures

Synthesis of NiS_2/CdS: NiS_2/CdS composite was prepared using the same procedure as shown in Fig. 1, except with $Cd(Ac)_2{\cdot}2H_2O$ and $Ni(NO_3)_2{\cdot}6H_2O$ both as metal precursors. The resulting solid was denoted as x% NiS_2/CdS, where x represents the calculated mole fraction of NiS_2.

Synthesis of NiS_2: Peony-like NiS_2 nanosheets were prepared using the same procedure, except with $Ni(NO_3)_2{\cdot}6H_2O$ (0.001 mol) as metal precursor.

Synthesis of NiS_2+CdS: NiS_2+CdS was prepared by two-step method. The as-prepared CdS (0.01 mol) was dispersed into PEG-based DES with $Ni(NO_3)_2{\cdot}6H_2O$ (0.001 mol), and the following operation method was exactly the same as mentioned above to obtain the precipitate (10 % NiS_2+CdS).

1.2. Characterization of photocatalysts

The X-ray powder diffraction (XRD) patterns of the products were recorded on D/max-2550/PC diffractometer (Rigaku) at 40 kV and 30 mA with Cu Kα as X-ray (λ =1.5418Å). SEM images, EDS spectra and elemental mapping images of the samples were obtained using a Hitachi SU 8010 field emission scanning electron microscope combined with energy dispersive X-ray spectroscopy at 15.0 kV. X-ray photoelectron spectroscopy (XPS) was carried out on an ESCALAB MK X-ray photoelectron spectrometer. The morphological and microstructural features of the samples were recorded by high-resolution transmission electron microscopy (HRTEM JEOL-2010). The diffuse reflectance spectra at room temperature were obtained using a UV-vis spectrophotometer (Hitachi U-4100) with $BaSO_4$ as a reflectance standard. The specific surface areas were analyzed using the BET method using the nitrogen adsorption-desorption instrument (JW-BK122W, China). Steady-state photoluminescence (PL) spectra and PL decay were performed using an Edinburgh FLS 980 transient steady-state spectrometer with a 375-nm laser. The carbon-centered radicals were detected on an electron paramagnetic resonance (EPR, Bruker EMXnano, Bruker, Germany).

1.3. Density functional theory (DFT) calculations

All the DFT calculations were carried out in the Vienna *ab initio* simulation (VASP5.4.4) code.[1] The exchange-correlation is simulated with PBE functional and the ion-electron interactions were described by the PAW method.[2, 3] The vdWs interaction was included by using empirical DFT-D3 method.[4] The Monkhorst-Pack-grid-mesh-based

Brillouin zone k-points are set as 2×2×1 for NiS_2 and CdS@NiS_2, while 3×3×1 for CdS periodic structure with the cutoff energy of 450 eV. The convergence criteria are set as 0.01 eV A^{-1} and 10^{-5} eV in force and energy, respectively. A at least 20 Å vacuum layer along the *z* direction is employed to avoid interlayer interference.

1.4. Electrochemical measurements

The electrochemical experiments analysis was performed using electrochemical workstation (Shanghai ChenHua Instrument Company). The counter electrode was made of platinum wire, and the reference electrode was made of Ag/AgCl in a saturated potassium chloride solution. The sample slurry was coated on an ITO glass substrate (the fixed area of ITO was 1·1 cm^2), and then the film was air-dried overnight to prepare a thin-film working electrode. Na_2SO_4 aqueous solution (1.0 M) was used as the electrolyte for measurements, and a 3 W monochromatic light source (k ¼ 420 nm) was the visible light source. Mott-Schotty analysis was in the potential range from 0 to 1.0 V (vs Ag/AgCl) with a frequency of 1kHz in the dark.

1.5. Electron paramagnetic resonance measurement

A 10 mg sample was scattered in 20 mL of HMF aqueous solution (0.1 M) containing a radical spin-trapping agent-5,5-dimethyl-1-pyrroline N-oxide (DMPO, 0.1 M). The suspension-filled glass capillary was placed in a sealed glass tube under an Ar

environment, and then placed in the microwave cavity of the EPR spectrometer, and irradiated at room temperature with a xenon lamp (420 nm).

2. Results and Discussion

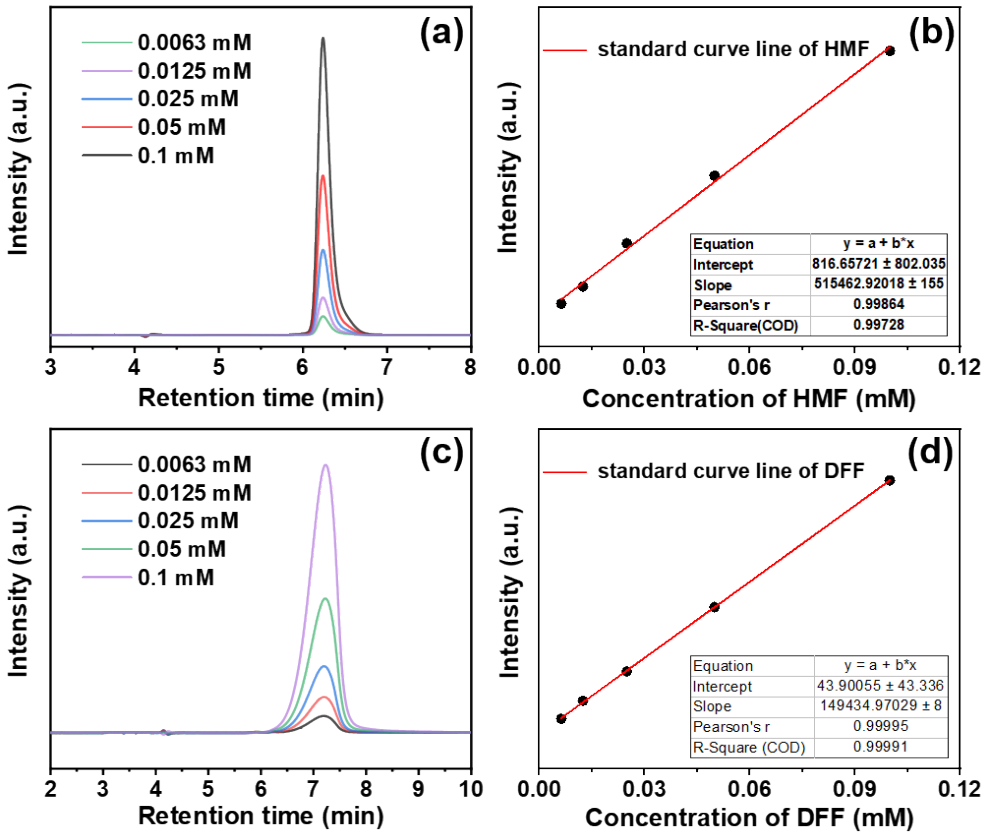

Fig. S1. HPLC measurements of HMF (a) and DFF (c); Standard curves of the HPLC for HMF (b) and DFF (d).

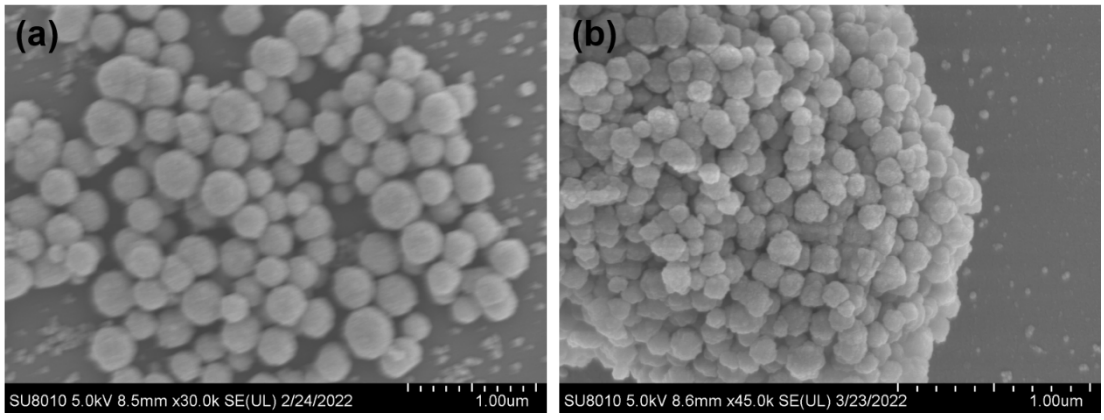

Fig. S2. SEM images of pure CdS (a) and 10 % NiS_2/CdS (b)

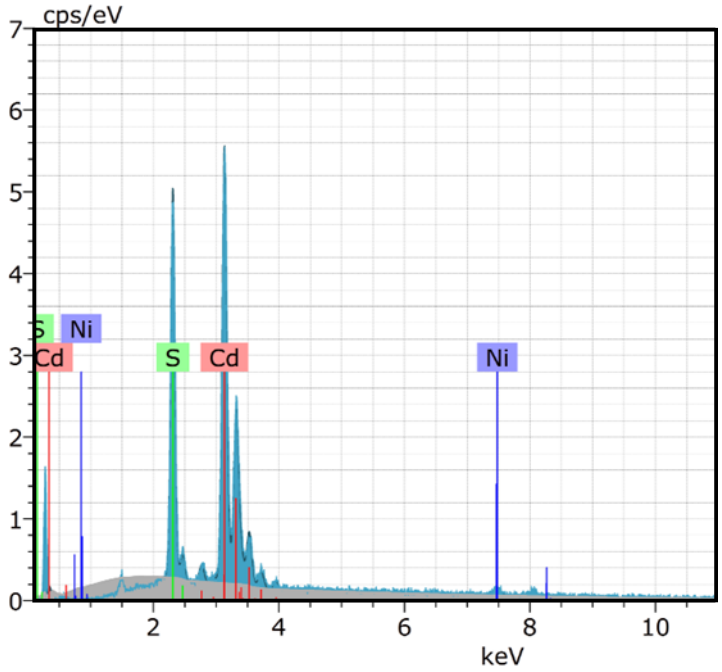

Fig. S3. EDS quantitative analysis of the as-prepared 10% NiS_2/CdS.

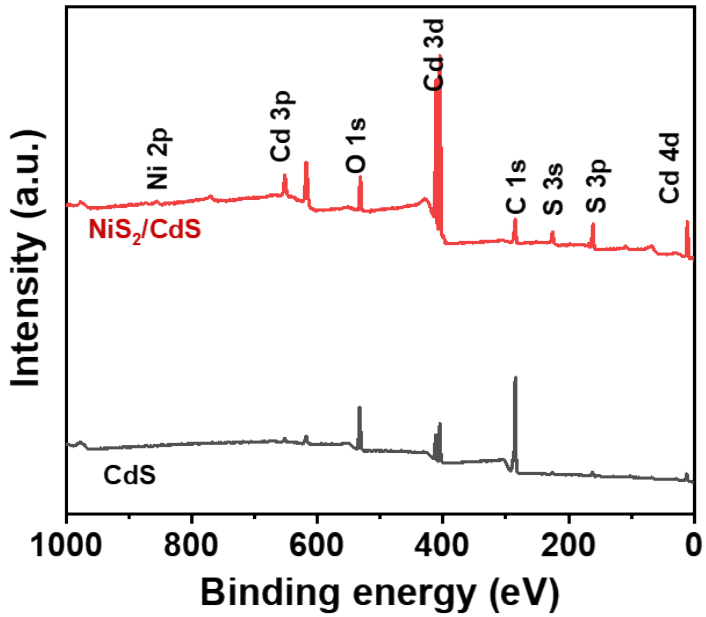

Fig. S4. XPS surface survey spectra of bare CdS and 10 % NiS_2/CdS

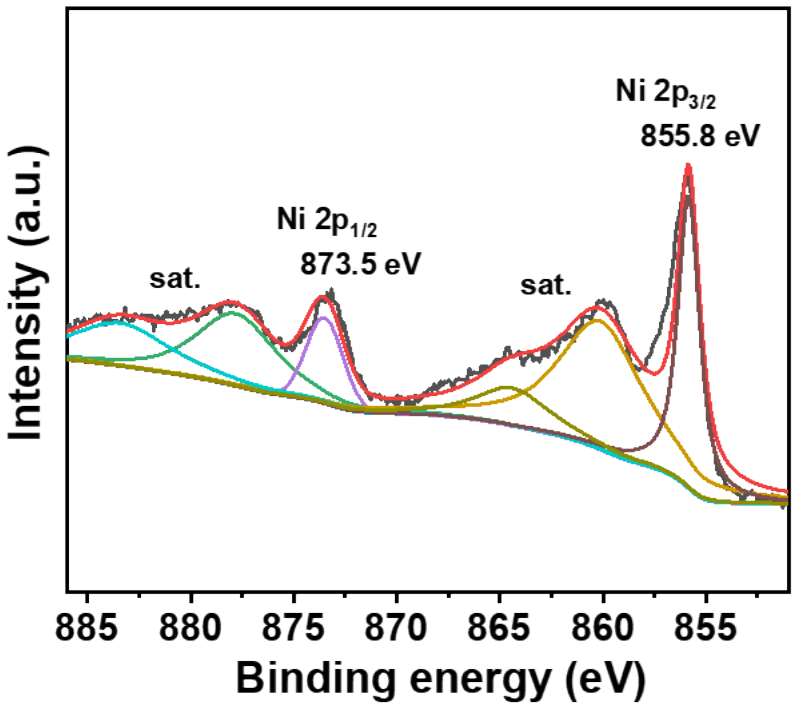

Fig. S5. Ni 2p spectrum of pristine NiS_2.

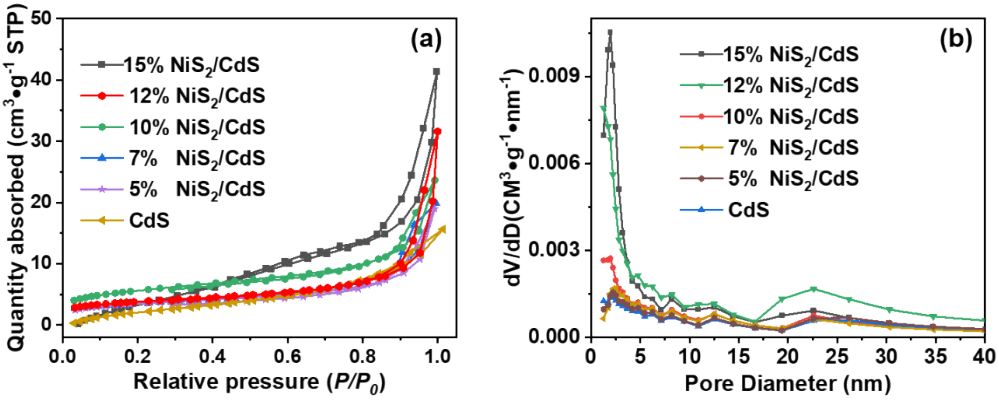

Fig. S6. N_2 adsorption–desorption isotherms (a) and pore-size distribution (b) of CdS and x% NiS_2/CdS.

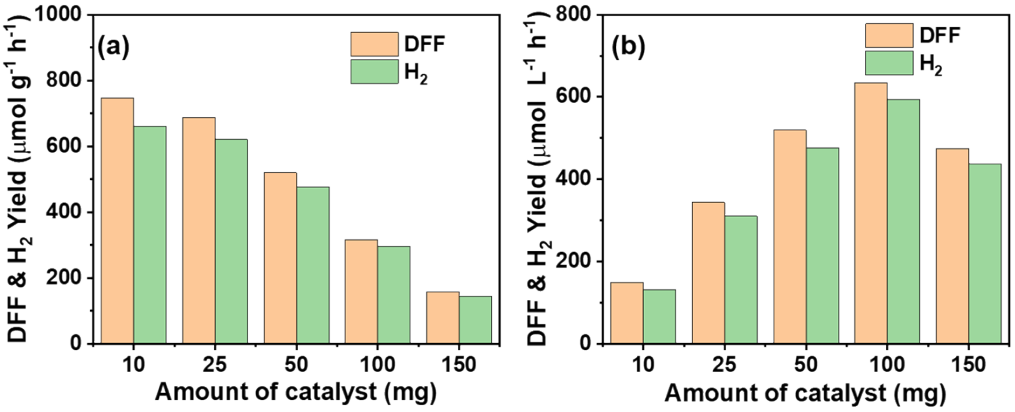

Fig. S7. Photocatalytic rates were measured on a per-unit-mass basis (a) and per-unit-volume basis(b).

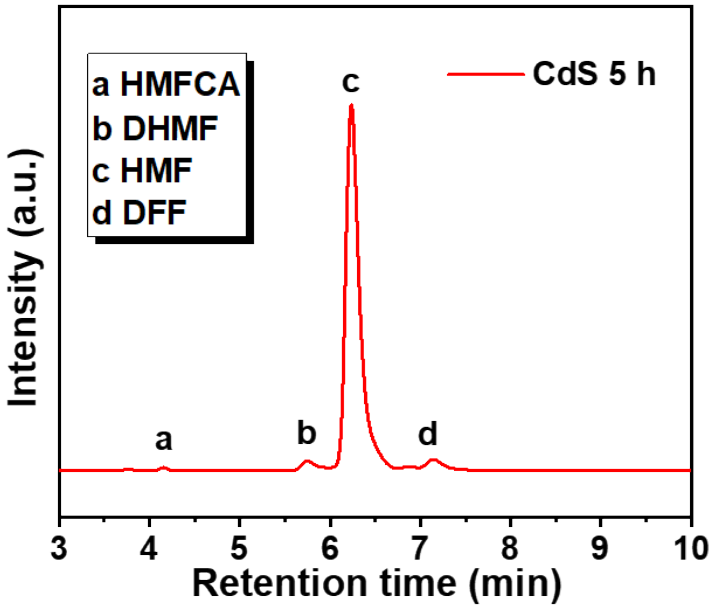

Fig. S8. HPLC traces of photocatalytic oxidation of HMF by CdS under visible light irradiation.

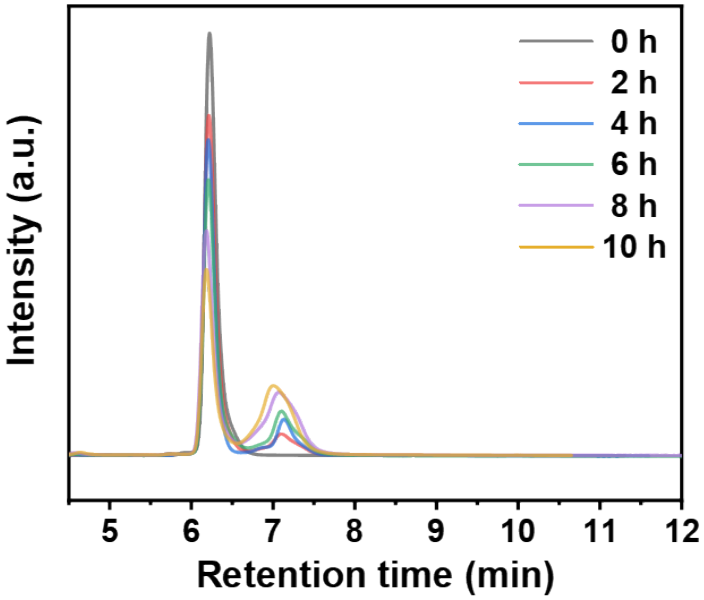

Fig. S9. HPLC traces of photocatalytic oxidation of HMF by 10% NiS_2/CdS.

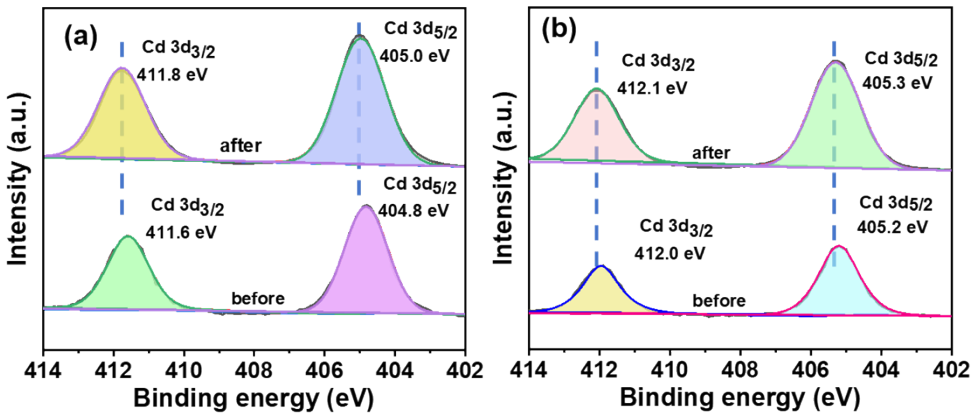

Fig. S10. Binding energy shift of Cd 3d in pure CdS (a) and 10% NiS_2/CdS (b) composite before and after photostability test.

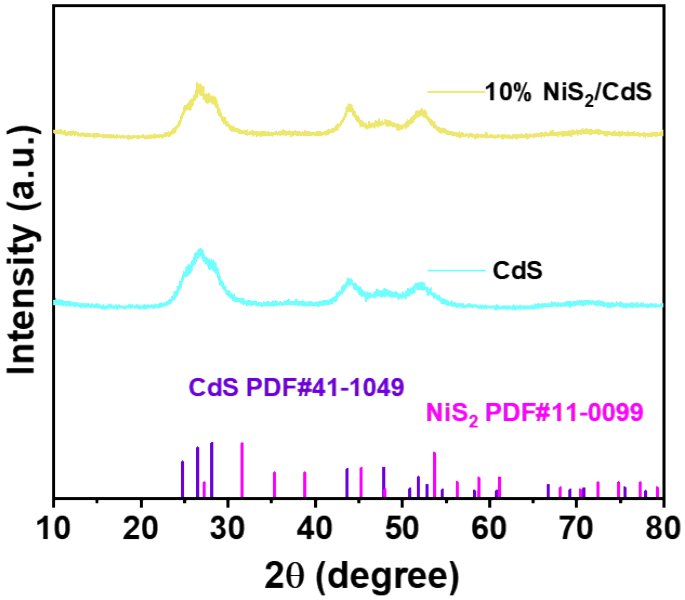

Fig. S11. XRD patterns of CdS and 10% NiS_2/CdS after photocatalysis.

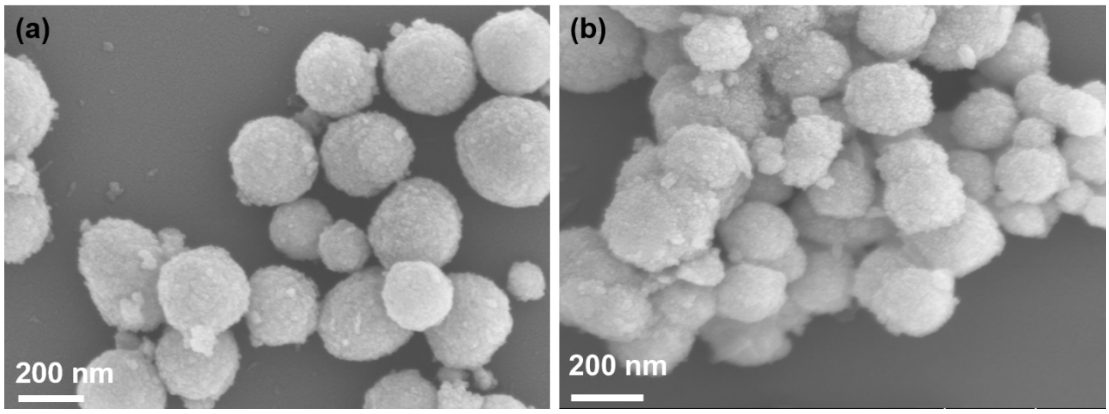

Fig. S12. SEM images of CdS (a) and 10% NiS_2/CdS (b) after photocatalysis.

Table S1. Results of the photocatalytic oxidation of HMF under both similar and different conditions.

PhotoCatalyst	Solvents	Reaction conditions	Products	Yield rate of DFF (μmol g^{-1} h^{-1})	Selectivity %	Ref.
NiS_2/CdS	water	(λ > 420 nm), under N_2	DFF, H_2	519.6	95.2	This work
g-C_3N_4	water	(λ > 420 nm), under N_2	DFF, H_2	95.0	97.0	[5]
NiS/$Zn_3In_2S_6$	Water	(λ > 400 nm), under N_2	DFF, H_2	120.0	94.1	[6]
CdxInyS(x+1.5y)	water	(λ > 420 nm), under air	DFF, FDCA	--	62.7	[7]
CuSAs/p-CNS	acetonitrile (90%) solution	(λ = 455 nm), under O_2	DFF	--	85.6	[8]
Ag/TiO_2	Na_2CO_3 solution	(λ > 420 nm), under O_2	HMFCA	--	96.7	[9]
SGH-TiO_2	acetonitrile	(λ = 515 nm), under air	DFF	--	87.0	[10]
$MAPbBr_3$	acetonitrile	(λ =450 nm), under air	DFF	--	90.0	[11]

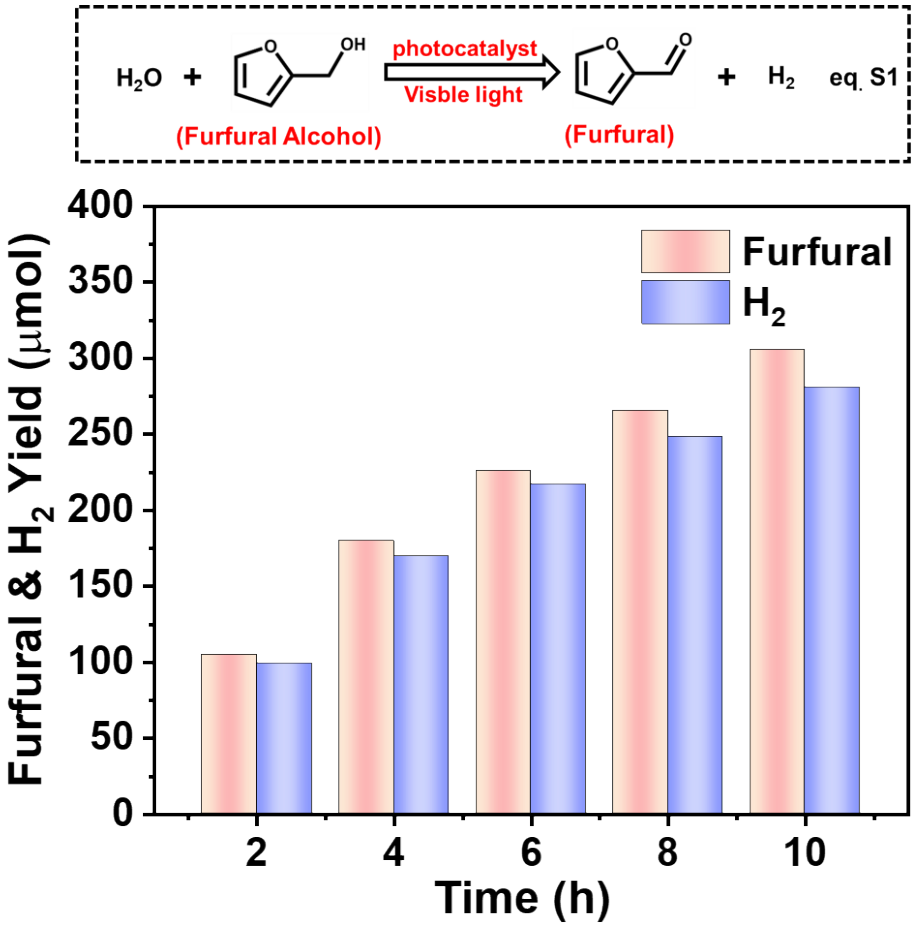

Fig. S13. Time-online photocatalytic selective transformation of furfural alcohol activity over the 10 % NiS_2/CdS sample.

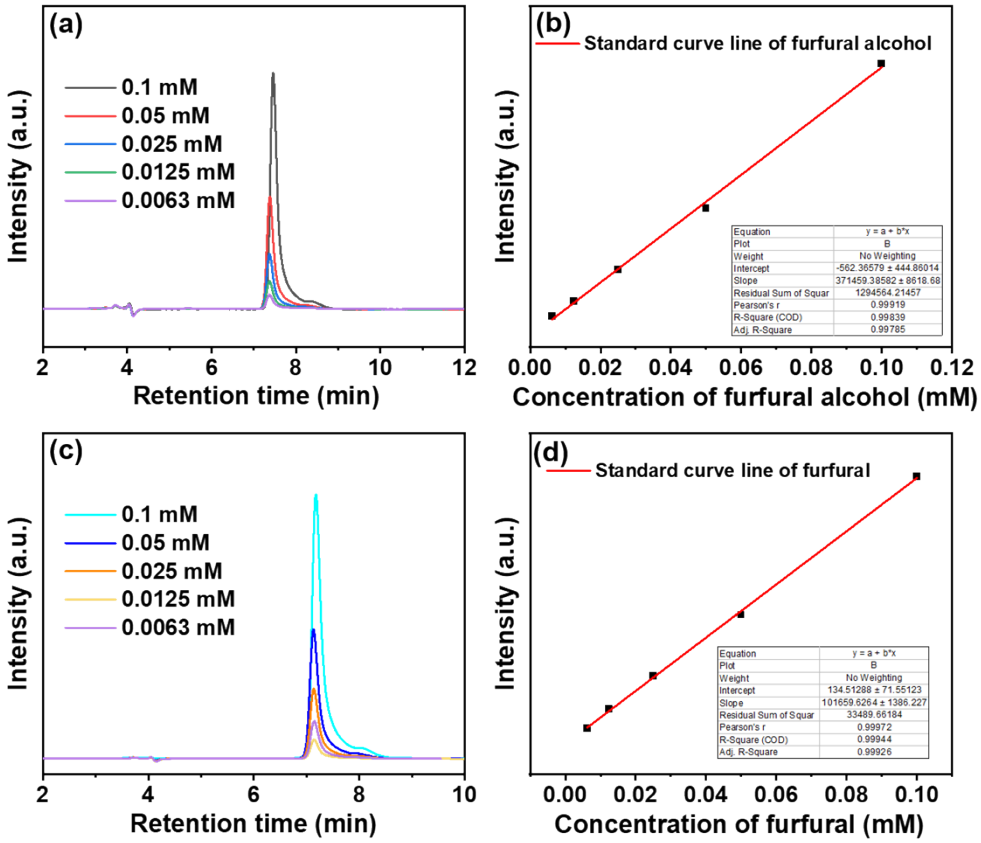

Fig. S14. HPLC measurements of furfural alcohol (a) and furfural (c); Standard curves of the HPLC for furfural alcohol (b) and furfural (d).

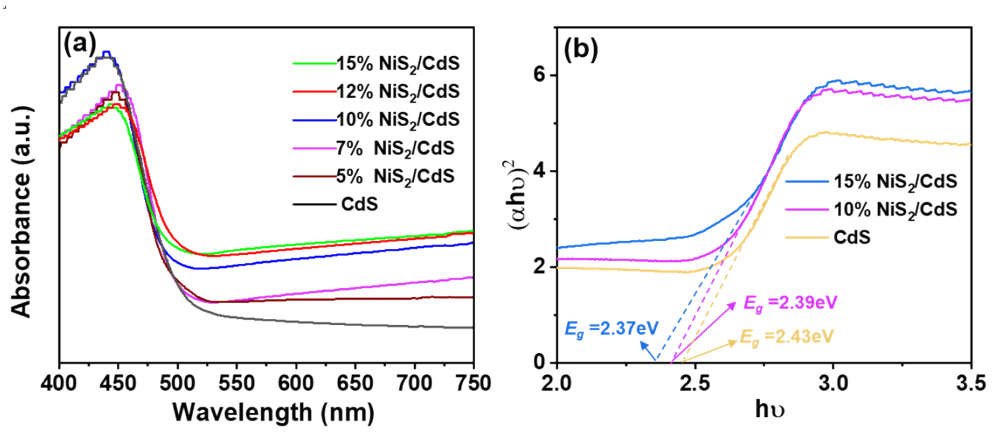

Fig. S15. UV–vis DRS spectra (a) and Kubelka-Munk-transformed reflectance spectra (b) of CdS and x% NiS_2/CdS samples.

Table S2. Band Gap (Eg) of 5 % NiS_2/CdS, 7 % NiS_2/CdS, 12 % NiS_2/CdS.

Sample	E_g (eV)
5% NiS_2/CdS	2.42 eV
7% NiS_2/CdS	2.41 eV
12% NiS_2/CdS	2.38 eV

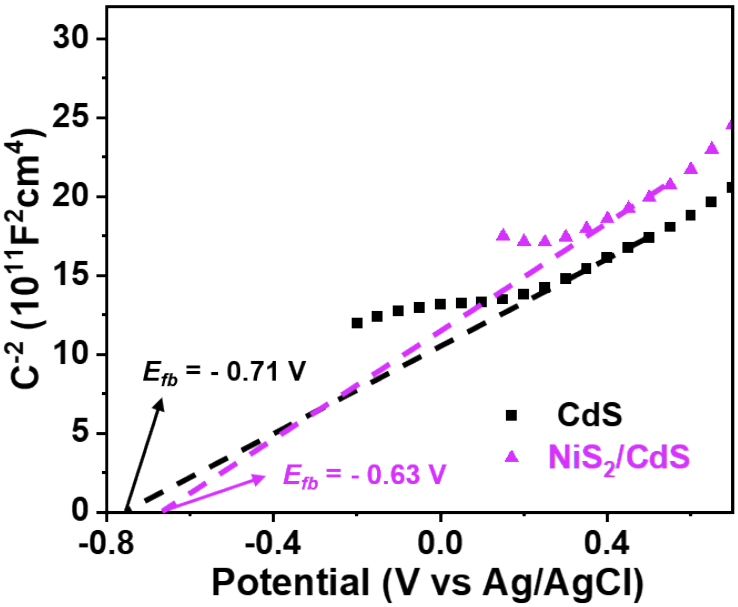

Fig. S16. Plots of transformed Kubelka-Munk function versus photon energy for CdS and NiS_2/CdS.

Table S3. Time-resolved photoluminescence decay parameters of pure CdS and 10 % NiS_2/CdS

Sample	Lifetime (τ) (ns)		Pre-exponential factor A%		τ_{ave} (ns)
	τ_1	τ_2	A_1	A_2	
CdS	1.06	9.05	95.82	5.20	3.58
NiS_2/CdS	0.64	3.83	84.58	18.43	2.45

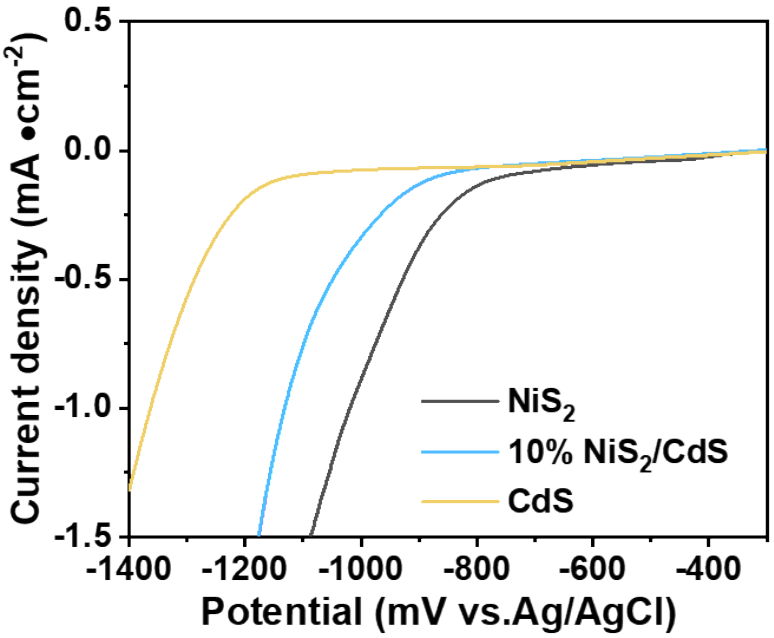

Fig. S17. LSV polarization curves.

References

1. G. Kresse and J. Furthmuller, *Phys. Rev. B*, 1996, **54**, 11169.
2. J. P. Perdew, K. Burke and M. Ernzerhof, *Phys. Rev. Lett.*, 1996, **77**, 3865.
3. B. Hammer, L. B. Hansen and J. K. Norskov, *Phys. Rev. B*, 1999, **59**, 7413.
4. S. Grimme, *J. Comput. Chem.*, 2006, **27**, 1787-1799.
5. X. Bao, M. Liu, Z. Wang, D. Dai, P. Wang, H. Cheng, Y. Liu, Z. Zheng, Y. Dai and B. Huang, *ACS Catalysis*, 2022, **12**, 1919-1929.
6. S. G. Meng, H. H. Wu, Y. J. Cui, X. Z. Zheng, H. Wang, S. F. Chen, Y. X. Wang and X. L. Fu, *Appl. Catal., B*, 2020, **266**, 118617.
7. M. Zhang, Z. Yu, J. Xiong, R. Zhang, X. Liu and X. Lu, *Appl. Catal., B*, 2022, **300**, 120738.
8. G. Wang, R. Huang, J. Zhang, J. Mao, D. Wang and Y. Li, *Adv. Mater.*, 2021, **33**, e2105904.
9. W. Zhang, X. Li, S. Liu, J. Qiu, J. An, J. Yao, S. Zuo, B. Zhang, H. Xia and C. Li, *ChemSusChem.*, 2022, **15**, 202102158.
10. A. Khan, M. Goepel, A. Kubas, D. Lomot, W. Lisowski, D. Lisovytskiy, A. Nowicka, J. C. Colmenares and R. Glaser, *ChemSusChem.*, 2021, **14**, 1351-1362.
11. M. Zhang, Z. Li, X. Xin, J. Zhang, Y. Feng and H. Lv, *ACS Catal.*, 2020, **10**, 14793-14800.